X-ray Diffraction Study of Ionic Liquid Based Mixtures

ARTICLE *in* THE JOURNAL OF PHYSICAL CHEMISTRY B · FEBRUARY 2009

Impact Factor: 3.3 · DOI: 10.1021/jp808883p · Source: PubMed

3 AUTHORS, INCLUDING:

Yusuke Imai
National Defense Academy of Japan
26 PUBLICATIONS **292** CITATIONS
SEE PROFILE

Hiroshi Abe
National Defense Academy of Japan
118 PUBLICATIONS **681** CITATIONS
SEE PROFILE

X-ray Diffraction Study of Ionic Liquid Based Mixtures

Yusuke Imai, Hiroshi Abe, and Yukihiro Yoshimura

J. Phys. Chem. B, **2009**, 113 (7), 2013-2018• Publication Date (Web): 26 January 2009

X-ray Diffraction Study of Ionic Liquid Based Mixtures

Yusuke Imai,[†] Hiroshi Abe,*[,†] and Yukihiro Yoshimura[‡]

Department of Materials Science and Engineering, and Department of Applied Chemistry, National Defense Academy, Yokosuka 239-8686, Japan

Received: October 7, 2008; Revised Manuscript Received: December 12, 2008

Crystal structures in *N*,*N*-diethyl-*N*-methyl-*N*-2-methoxyethylammonium tetrafluoroborate, [DEME][BF_4], are determined by X-ray diffraction method. In [DEME][BF_4]-based mixtures, various kinds of crystal structures and superstructures are induced by additives, i.e., H_2O, CH_3OH, C_2H_5OH, and C_6H_6. Most of the crystal structures in the mixtures are related to that of pure [DEME][BF_4], though unit cells in 1.1 and 6.1 mol % C_6H_6 are different from the pure one. Further, [DEME][BF_4]−C_6H_6 mixtures require the two kinds of superstructures, where volume per [DEME][BF_4] is contracted by a small amount of additives. Also, volume contraction and the coexistence of two kinds of superstructures are seen in 0.9 mol % H_2O. The superstructures are derived from orientational or displacive modulations of [DEME][BF_4] molecules. In spite of a small amount of additives, molecular interactions of [DEME][BF_4] are influenced extensively.

1. Introduction

Molecular room temperature ionic liquids (RTILs) have been the subjects of environmentally "green" chemistry.[1] Their vapor pressure is almost zero. Therefore, RTILs are widely applied into organic synthesis and separation chemistry. On the other hand, as a scientific interest, many studies of crystal structures are carried out in order to clarify the molecular interactions in RTILs. Two kinds of crystal structures (I + II) were found in pure 1-butyl-3-methylimidazolium chloride, [C_4mim]Cl, by X-ray powder patterns.[2] By isothermal holding at −18 °C, the coexistent phase (I + II) transformed to stable phase (II). Therefore, phase (I) was regarded as a metastable phase. Further structural study was performed using single crystals of [C_4mim]Cl[3] and [C_4mim]Br.[4] Crystal structure of [C_4mim]Cl is determined to be monoclinic ($P2_1/n$, $Z = 4$). It is considered that each chloride anion is hydrogen-bonded to three different imidazolium cations. On the other hand, the crystal structure of [C_4mim]Br is found to be orthorhombic ($Pna2_1$, $Z = 4$). In [C_4mim]-based mixtures, additional monoclinic structure appeared.[5] Pure [C_4mim]Cl and [C_4mim]Br are assigned as orthorhombic ($Pna2_1$, $Z = 4$). The mixtures of [C_4mim]Cl and [C_4mim][PF_6], [C_4mim]Cl and [C_4mim][BF_4], or [C_4mim]Cl/benzene and [C_4mim]Cl/toluene clathrates cause (II) monoclinic ($P2_1/c$, $Z = 4$). On the other hand, 1,3-dimethylimidazolium hexafluorophosphate, [C_1mim][PF_6] and [C_1mim][PF_6]−50 mol % C_6H_6 were investigate to obtain π-electron effect in the RTIL.[6] The cation in the pure RTIL forms zigzag chains. In contrast, the RTIL−C_6H_6 mixture shows cation−benzene "sandwich" packing. The peculiar feature is that the benzene molecules do not interact with others. The benzene is isolated by the RTIL network.

In molecular dynamics simulations,[7] water behavior in [C_1mim]Cl and [C_1mim][PF_6] was simulated. The local structure and the dynamics of the mixtures were analyzed over the wide range of water concentration. In the RTIL-rich phase, water molecules tend to be isolated from each other in the mixtures, although a continuous water network appears in the water-rich phase. In radial distribution functions, the first peak, which is derived from anions of hydrogen-bonded to water molecules, becomes sharper and higher when the water content is small. Advanced molecular dynamics simulations show the significant nanostructual organization in 1-octyl-3-methylimidazolium nitrate RTIL−water mixtures.[8] Nonpolar and polar phase separation occurs on nanoscale. Each polar region is linked by a water molecule in RTIL-rich phase.

Recently, *N*,*N*-diethyl-*N*-methyl-*N*-2-methoxyethylammonium tetrafluoroborate, [DEME][BF_4], as a different kind of RTIL was synthesized for electrochemical capacitors, which has a quite wide potential window.[9] Fundamental physical properties of [DEME][BF_4] were evaluated. In addition, anomalous domain growth was observed in [DEME][BF_4]−H_2O mixtures.[10] Here, three different types of the domain structures were formed with a small content of H_2O. The anomalous domain growth is not seen in [DEME][BF_4]−CH_3OH, −C_2H_5OH, and −C_6H_6. On the other hand, the complicated phase diagram in [DEME][BF_4]−H_2O mixtures is determined by simultaneous X-ray diffraction and DSC measurements.[11] Below 4 mol % H_2O, crystal phase (C-phase) is formed on cooling. Amorphous phase (A-phase) appears from 4 to 10 mol % H_2O. Above 10 mol %, two-phase coexistence, (A + C)-phase, is observed. Upon heating, cold crystallization occurs above 4 mol % H_2O. Also, pure A-phase is characterized by "two different dynamic components" in Raman spectra, where the lower Raman band is crystal-like and the higher one is liquid-like.

In this study, we have determined crystal structures of [DEME][BF_4] based mixtures by X-ray diffraction method. [DEME][BF_4]−H_2O, −alcohols, and −C_6H_6 mixtures are investigated to obtain the effect of hydrogen bonding and π-electron. Moreover, H_2O and alcohols are regarded to have different types of hydrogen bonding. We have found that by addition of a few mol % of H_2O or C_6H_6, two kinds of superstructures and volume contractions are caused drastically, although alcohol contribution to [DEME][BF_4] is quite small.

* To whom correspondence should be addressed.
[†] Department of Materials Science and Engineering.
[‡] Department of Applied Chemistry.

10.1021/jp808883p CCC: $40.75
Published on Web 01/26/2009

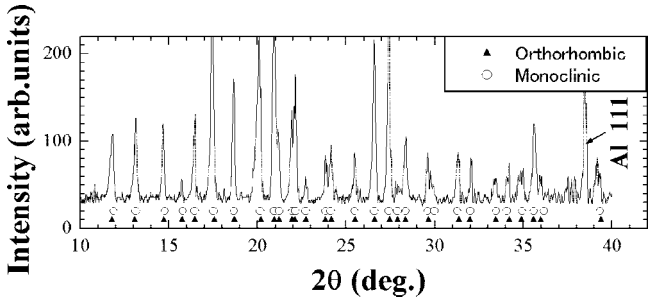

Figure 1. X-ray diffraction pattern at −80 °C ($T < T_c$) of pure ionic liquid [DEME][BF_4]. Crystal structure is assigned by monoclinic or orthorhombic. Open circles and closed triangles correspond to the calculated 2θ values of monoclinic and orthorhombic, respectively.

2. Experiments

We selected [DEME][BF_4] (Kanto Chemical Co.) as a RTIL. Since this RTIL is hydrophilic, 126 ppm H_2O is included in the as-received sample. Generally, the RTILs are contaminated easily by vacuum drying to reduce H_2O; thus, we used the sample without further purification. As additions to [DEME][BF_4], H_2O (0.6, 0.9, 2.9, 4.4, 8.8, and 12.0 mol %), CH_3OH (0.8 and 7.3 mol %), C_2H_5OH (1.2 and 6.7 mol %), and C_6H_6 (1.1 and 6.1 mol %) were prepared. Concentrations of 1 and 6 mol % were chosen because [DEME][BF_4]−0.9 mol % H_2O show the anomalous domain growth[10] and 6.7 mol % H_2O possesses pure A-phase.[11] For mixtures, we used distilled water, CH_3OH, C_2H_5OH, and C_6H_6 (Wako Pure Chemical Co.).

In situ observations were performed using X-ray diffraction and DSC. DSC was attached on a vertical goniometer with a 3 kW X-ray generator (RINT-Ultima III, Rigaku Co.). For in situ observations of liquid, a sample stage was fixed horizontally. A sealed X-ray tube and a scintillation counter moved simultaneously. Parallel beam was obtained by parabolic multilayer mirror. A long Soller slit was placed in front of scintillation counter. Cu Kα radiation ($\lambda = 0.1542$ nm) was selected for the simultaneous measurements. During simultaneous measurements, dry N_2 gas was flowing at 20 cm^3/min in order to reduce moisture. In this beam optics, beam divergence is estimated to be 0.1° by measuring a standard Si polycrystal. Also, the observed 2θ values are corrected by using those of a standard Si polycrystal. After corrections, the observed 2θ value of Al 111 Bragg reflection is in good agreement with the observed one within 0.03°, where Al is used as a sample holder. Crystal structures and precise lattice constants are determined by JADE application software (Rigaku Co.).

3. Results

3.1. Crystal Structures of Pure [DEME][BF_4]. At first, the crystal structure of pure [DEME][BF_4] was determined by X-ray diffraction method. Figure 1 shows diffraction pattern of pure [DEME][BF_4] at −80 °C. Here, the crystallization temperature, T_c, is found to be around −30 °C by simultaneous X-ray and DSC measurements.[10] 2θ values of Bragg reflections are fitted well by monoclinic or orthorhombic. Open circles and closed triangles reveal the calculated values of monoclinic and orthorhombic ones, respectively. The calculated peak positions are in good agreement with the observed ones within 0.12°. The judgment is based on the average full width at half-maximum (fwhm) of Bragg reflections (0.15°−0.20°) and beam divergence (0.1°). Since the preferred orientation of Bragg reflections is not negligible,[10] we argue the peak positions without considering Bragg intensities. Monoclinic lattice has a relation with orthorhombic (Figure 2a). For a comparison, molecular size is illustrated in Figure 2b. a_M, b_M, c_M, a_O, b_O, and c_O are lattice constants of monoclinic and orthorhombic ones, respectively. The relation between the lattice parameters of monoclinic and orthorhombic is $\mathbf{a}_M \approx \mathbf{b}_O - \mathbf{c}_O$, $\mathbf{b}_M \approx \mathbf{a}_O$, and $\mathbf{c}_M \approx \mathbf{c}_O$. Space group of monoclinic is found to be $P2_1$ with $a_M = 1.632$, $b_M = 1.009$, $c_M = 0.896$ nm, and $\beta = 123.8°$. Orthorhombic space group is *Pbcm* with $a_O = 1.012$, $b_O = 1.347$, and $c_O = 0.893$ nm. Here, the density of pure [DEME][BF_4] is estimated to be 1.17 g/cm^3.[9] Calculated density using the above lattice constants and $Z = 4$ is found to be 1.26 g/cm^3. Furthermore, the orthorhombic lattice has a peculiar geometric relation, which is given by

$$2b_O = 3c_O = 2\sqrt{{a_O}^2 + {c_O}^2} \quad (1)$$

If we consider a sublattice, which has the equivalent length (2.7 nm) of a sublattice constant, the sublattice contains 48 molecules of [DEME][BF_4].

3.2. Crystal structures of [DEME][BF_4]−H_2O mixtures. In the previous study,[10] it was found that water's effect on [DEME][BF_4] is not negligible on nucleation and growth process. X-ray diffraction patterns of [DEME][BF_4]−0.6, −0.9,and −2.9 mol % H_2O are shown in Figure 3, a, b, and c, respectively. Bragg peaks of 0.6 and 2.9 mol % H_2O are assigned by those of pure [DEME][BF_4]. However, X-ray diffraction pattern of 0.9 mol % H_2O is obviously different from pure, 0.6 and 2.9 mol % H_2O mixtures. If we assume smaller unit cell and two different kinds of modulated structures (superstructures), the observed 2θ values are the almost same as the calculated ones. Smaller unit cell of orthorhombic is expressed by $a'_O = 1.08$, $b'_O = 1.34$, and $c'_O = 0.78$. Open squares represent supercell of $a'_O \times b'_O \times 2c'_O$ ($Z = 8$), while open triangles exhibit another supercell of $2a'_O \times b'_O \times 2c'_O$ ($Z = 16$) (Figure 3b). Unit cells and lattice parameters of further H_2O contents in the mixtures are summarized in Tables 1 and 2, respectively. Crystal structures of the mixtures in 4.4, 8.8, and 12.0 mol % H_2O are explained using unit cell of pure [DEME][BF_4]. In the previous study,[11] pure A-phase exists from 4 to 10 mol % H_2O and (A + C)-phase is formed above 10 mol % H_2O. Here, crystal structure above 4 mol % is determined using X-ray diffraction data after "cold crystallization" on heating. On another approach to clarify the anomalous crystal structure of 0.9 mol % H_2O, H_2O dependence of volume per four [DEME][BF_4], V_4, is calculated as shown in Figure 4. It is necessary to normalize unit cell, V_c, by the number of molecules inside V_c, since [DEME][BF_4]−0.9 mol % H_2O mixture possesses a supercell based on the unit cell of the pure one. H_2O concentration dependence of V_4 is shown in Figure 4. V_c is obtained using the refined lattice constants. Open circle indicates normal V_4 ($Z = 4$). At 0.9 mol %, supercells are expressed by $2V_4$ (closed triangles) and $4V_4$ (closed squares). It should be stressed that, within a little amount of H_2O additions, a lattice expansion is not perceptible in the mixtures, which are described by V_4. In contrast, distinct volume contractions are observed only at 0.9 mol % H_2O, which has supercells. In particular, it has a tendency that a larger unit cell shows larger contraction.

3.3. Crystal Structures of Other Mixtures. Other additions also contribute to [DEME][BF_4] more or less. As other additions in the mixtures, we select CH_3OH, C_2H_5OH, and C_6H_6. Apart from [DEME][BF_4]−H_2O mixtures, [DEME][BF_4]−CH_3OH, −C_2H_5OH, and −C_6H_6 mixtures have no A-phase around 7 mol %. At first, [DEME][BF_4]−CH_3OH mixtures show different

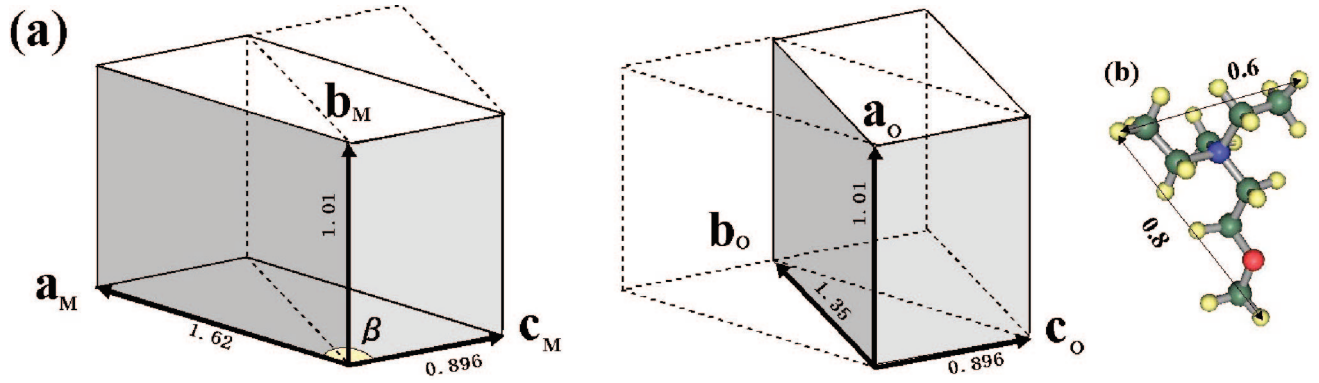

Figure 2. (a) Two kinds of unit cells. (b) Molecular structure of cation, [DEME]. Each unit cell has a relation each other. a_M, b_M, and c_M reveal lattice constants of monoclinic, and a_O, b_O, and c_O exhibit those of orthorhombic.

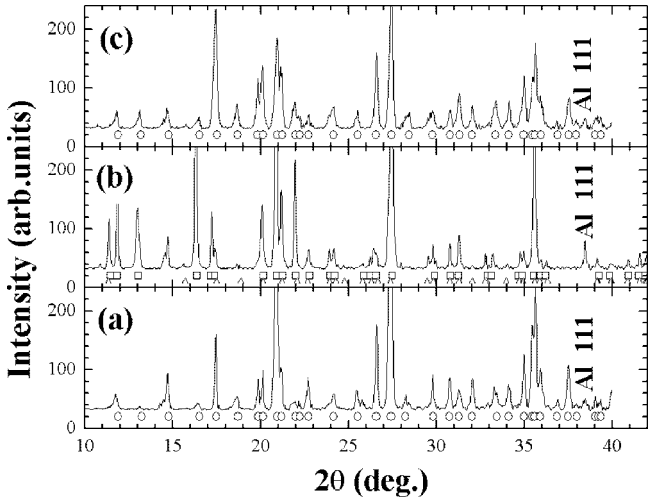

Figure 3. X-ray diffraction patterns of [DEME][BF_4]−H_2O mixtures depend on additions. Crystal structures of (a) 0.6 mol %, (b) 0.9 mol %, and (c) 2.9 mol % H_2O are calculated. Only the crystal structure of 0.9 mol % H_2O is not calculated by unit cells of pure [DEME][BF_4]. Open squares reveal $a'_O \times b'_O \times 2c'_O$ modulated lattice and open triangles exhibit $2a'_O \times b'_O \times 2c'_O$ modulated lattice.

X-ray diffraction patterns (Figure 5a,b). For instance, the crystal structure of [DEME][BF_4]−0.8 mol % CH_3OH is determined to be orthorhombic, which is connected with that of pure [DEME][BF_4] ($a_O \times b_O \times c_O$). In contrast, [DEME][$BF_4$]−7.3 mol % CH_3OH possesses a supercell, which is described by $a_O \times b_O \times 2c_O$ ($Z = 8$). The different modulation of anions or cations is caused by the specified CH_3OH addition. On the other hand, crystal structures of [DEME][BF_4]−C_2H_5OH mixtures are explained by unit cells based on pure ones (Figure 6a,b). For instance, [DEME][BF_4]−1.2 and −6.7 mol % C_2H_5OH are assigned by orthorhombic ($a_O \times b_O \times c_O$) and monoclinic ($a_M \times b_M \times c_M$), respectively. In contrast to previous mixtures, an entirely different crystal structure is found in [DEME][BF_4]−C_6H_6 mixtures. Complicated X-ray diffraction patterns of the [DEME][BF_4]−C_6H_6 are shown in Figure 7, a (1.1 mol %) and b (6.1 mol %). In fact, it is not possible to index using unit cells of pure [DEME][BF_4]. If we introduce different monoclinic unit cell ($a'_M \times b'_M \times c'_M$) as illustrated in Figure 8 and its modulated lattice, we can succeed in analyzing even in complicated X-ray diffraction patterns. The relation between the lattice parameters of monoclinic and orthorhombic is $\mathbf{a}'_M \approx \mathbf{b}_O - \mathbf{a}_O$, $\mathbf{b}'_M \approx \mathbf{c}_O$, and $\mathbf{c}'_M \approx \mathbf{a}_O$. a'_M, b'_M, c'_M, and β are 1.69, 0.896, and 1.01 nm and 126.7°, respectively. It is clear that the monoclinic unit cell ($a'_M \times b'_M \times c'_M$) has another orientational relation with orthorhombic one ($a_O \times b_O \times c_O$) of pure [DEME][$BF_4$]. In fact, [DEME][$BF_4$]−1.1 mol % C_6H_6 consists of $a_O \times b_O \times c_O$ and $a'_M \times 2b'_M \times 2c'_M$. Open circles in Figure 7a indicate a supercell ($a'_M \times 2b'_M \times 2c'_M$, $Z = 16$), while closed triangles are orthorhombic ($a_O \times b_O \times c_O$). At 6.1 mol % C_6H_6, the complicated diffraction pattern such as 1.1 mol % C_6H_6 is not seen (Figure 7b). One simple crystal ($a'_M \times b'_M \times c'_M$) is sufficient to explain the observed diffraction pattern. Just comparing between [DEME][BF_4]−H_2O and −C_6H_6 mixtures around 1 mol %, it is noticed that both of them have two kinds of superstructures. Supercells of all mixtures along with those of [DEME][BF_4]−H_2O are summarized in Table 1. Also, lattice parameter values of unit cell are listed in Table 2.

In the same manner as with the [DEME][BF_4]−H_2O system, the mass effect of all additions is investigated by calculating the volume per four [DEME][BF_4], V_4. We assume mass parameter, xM, in order to compare each addition directly, where x is concentration and M is molecular weight of each addition. Except for 0.9 mol % H_2O and 1.1 mol % C_6H_6, V_4 has no relation with the mass parameters (Figure 9).

4. Discussion

We have found significant properties of additions in the [DEME][BF_4]-based mixtures. In general, additions provide the chemical internal stress on the lattice, where lattice distortions appear more or less. Then, lattice expansion becomes large proportionally to concentrations of additions. In [DEME][BF_4]-based crystals, such lattice expansion or distortion is suppressed unnaturally. Certainly, no peak broadening of Bragg reflections is observed in the mixtures. Instead of lattice expansion, the mixtures only of 0.9 mol % H_2O and 1.1 mol % C_6H_6 show extraordinary lattice contraction with accompanying symmetry breaking. In the other binary molecular system, that is, $C_7H_{12}O_4$−$C_6H_{12}N_4$,[12] phase transitions to superstructure and ferroelastic twinned domains occur with lattice contraction. Two steps of phase transitions are explained by stacking sequence of elementary layers, not by the chain orientations. In that system, competitive interaction, which destroys or rearranges the hierarchy of correlations, varies with increasing the number of C atoms in the C chain. Compared with $C_7H_{12}O_4$−$C_6H_{12}N_4$, we emphasize coexistence of two crystal structures including superstructure without strains and lattice distortions in 0.9 mol % H_2O and 1.1 mol % C_6H_6. Moreover, only 1% additions can contribute to long-range order of [DEME][BF_4]. At least, trivial H_2O additions have two roles for cation and anion ordering considering two kinds of crystal structures, which are different from pure [DEME][BF_4]. Here, it should be noticed that 0.9

TABLE 1: Each Unit Cell in the [DEME][BF_4] Mixtures Expressed by Lattice Constant of Pure [DEME][BF_4], where a_M, b_M, and c_M Exhibit Lattice Constants of Monoclinic, and a_O, b_O, and c_O Indicate Those of Orthorhombic, a'_O, b'_O, and c'_O Being Smaller Lattice Constants[a]

H_2O					
0.6%	0.9%	2.9%	4.4%	8.8%	12.0%
$a_O \times b_O \times c_O$	$a'_O \times b'_O \times 2c'_O$ $2a'_O \times b'_O \times 2c'_O$	$a_O \times b_O \times c_O$	$a_O \times b_O \times c_O$ $a_O \times b_O \times 2c_O$	$a_O \times b_O \times c_O$	$a_O \times b_O \times c_O$

CH_3OH		C_2H_5OH		C_6H_6	
0.8%	7.3%	1.2%	6.7%	1.1%	6.1%
$a_O \times b_O \times c_O$	$a_O \times b_O \times 2c_O$	$a_O \times b_O \times c_O$	$a_M \times b_M \times c_M$	$a_O \times b_O \times c_O$ $a'_M \times 2b'_M \times 2c'_M$	$a'_M \times b'_M \times c'_M$

[a] The monoclinic unit cell described by a'_M, b'_M, and c'_M has different orientational relation with the pure one (Figure 8).

TABLE 2: Lattice Parameters Determined by X-ray Diffraction Method[a]

additive	x (mol %)		a (nm)	b (nm)	c (nm)	β (deg)
H_2O	0.0	M	1.632	1.009	0.896	123.8
		O	1.012	1.347	0.893	
	0.6	O	1.013	1.338	0.893	
	0.9	O	1.096	1.356	1.542	
		O	2.122	1.331	1.560	
	2.9	O	1.012	1.341	0.892	
	4.4	O	1.013	1.343	0.892	
		O	1.013	1.338	1.785	
	8.8	O	1.012	1.346	0.893	
	12.0	O	1.014	1.348	0.892	
CH_3OH	0.8	O	1.012	1.337	0.892	
	7.3	O	1.007	1.356	1.781	
C_2H_5OH	1.2	O	1.012	1.345	0.892	
	6.7	M	1.609	1.016	0.891	123.9
C_6H_6	1.1	O	1.011	1.349	0.891	
		M′	1.678	1.748	2.070	128.5
	6.1	M′	1.701	0.888	1.023	128.1

[a] O, M, and M′ reveal orthorhombic, monoclinic, and a different kind of monoclinic, respectively. The respective lattice relations are drawn in Figures 2 and 8.

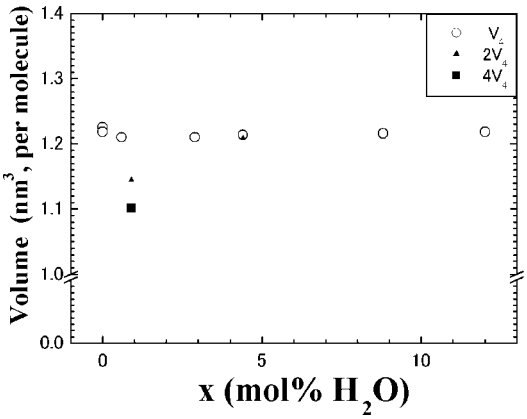

Figure 4. H_2O concentration dependence of volume per [DEME][BF_4], V_4. Modulated lattices such as $2V_4$ and $4V_4$ are normalized by the number of molecules for a comparison. V_4 at 0.9 mol % H_2O is extraordinary small.

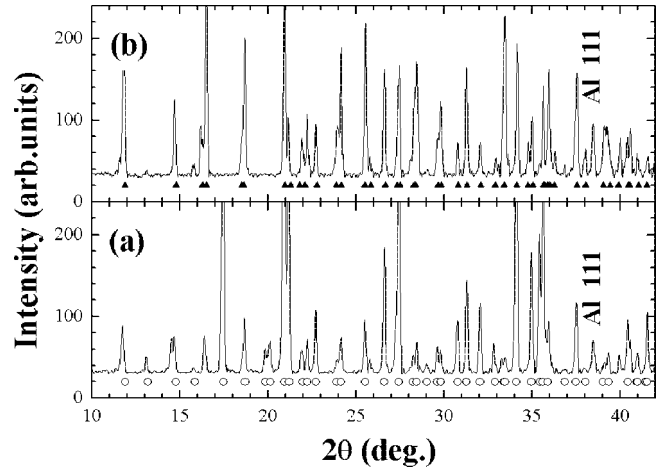

Figure 5. X-ray diffraction patterns of (a) 0.8 mol % and (b) 7.3 mol % CH_3OH. Open circles reveal orthorhombic lattice pf pure [DEME][BF_4]. [DEME][BF_4]−7.3 mol % CH_3OH has the modulated lattice based on unit cell of pure [DEME][BF_4]. Closed triangles are calculated by $a_O \times b_O \times 2c_O$.

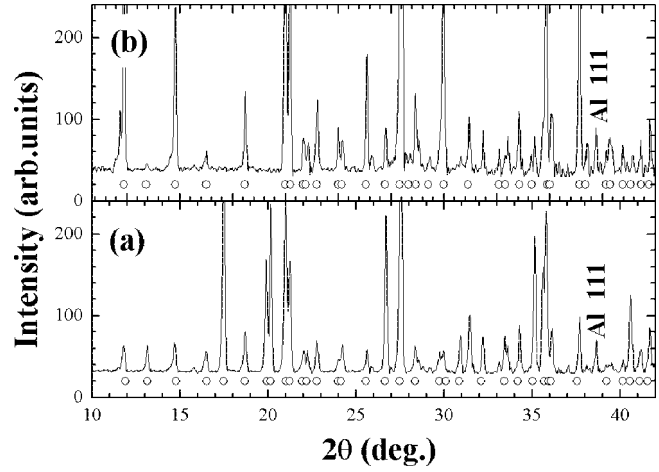

Figure 6. X-ray diffraction patterns of (a) 1.2 mol % and (b) 6.7 mol % C_2H_5OH. Open circles of 1.2 mol % and 6.7 mol % are calculated 2θ values using $a_O \times b_O \times c_O$ and $a_M \times b_M \times c_M$, respectively.

mol % H_2O possesses twined domains.[10] We conclude that 0.9 mol % H_2O shows anomalous elastic and structural behaviors.

Why are the mixtures of about 1 mol % H_2O or C_6H_6 so unusual? We gave a plausible explanation of the RTIL with water and benzene from a standpoint at the molecular level as below. On the basis of eq 1, we introduce a sublattice as shown in Figure 10. The sublattice consists of $2b_O$, $3c_O$, and $2[a_O^2 + c_O^2]^{1/2}$, where each sublattice parameter is 2.7 nm. Two sets of sublattice contain $24V_4$. Therefore, 96 molecules of [DEME][BF_4] are located in two sets of the sublattice. If one H_2O molecule exists inside two sets of the sublattice, 1/(1 + 96) provides 1.03 mol %. This means that the average distance of 1 mol % additives is equal to the sublattice parameters. For instance, one molecule can occupy sites at $P_1-P_2-Q_1-Q_2$, P_0-P_3, and $Q_1-Q_2-P_3$ on the sublattice points as shown in Figure 10. Since the lengths of P_0Q_1 and P_0Q_2 are too short,

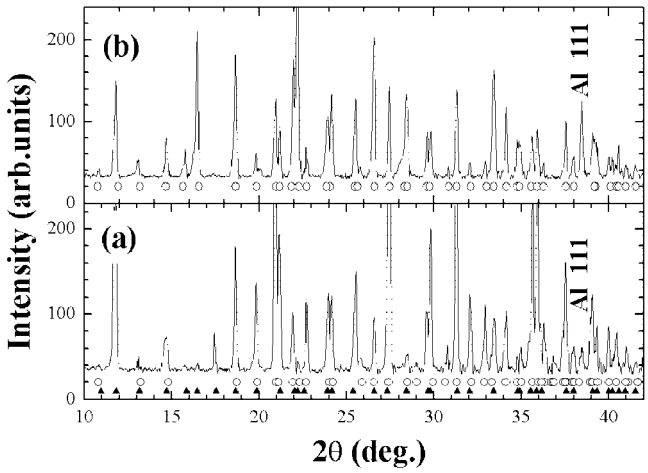

Figure 7. X-ray diffraction patterns of (a) 1.1 mol % and (b) 6.1 mol % C_6H_6. Highly modulated lattice and different monoclinic unit cell are required to explain the complicated X-ray diffraction pattern of 1.1 mol %. The different monoclinic lattice ($a'_M \times b'_M \times c'_M$) is shown in Figure 8. Open circles and closed triangles in Figure 7a shows modulated lattice ($a'_M \times 2b'_M \times 2c'_M$) and orthorhombic ($a_O \times b_O \times c_O$). At 6.1 mol %, only simple monoclinic lattice ($a'_M \times b'_M \times c'_M$) is enough to fit the X-ray diffraction pattern as shown in Figure 7b.

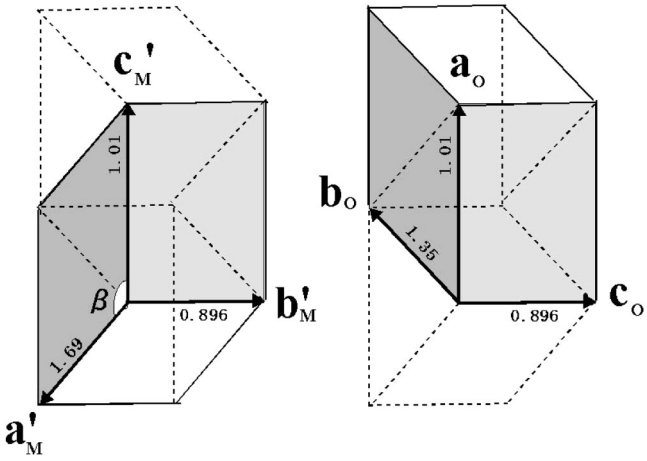

Figure 8. Different monoclinic lattice ($a'_M \times b'_M \times c'_M$) has orientational relation with the orthorhombic one ($a_O \times b_O \times c_O$).

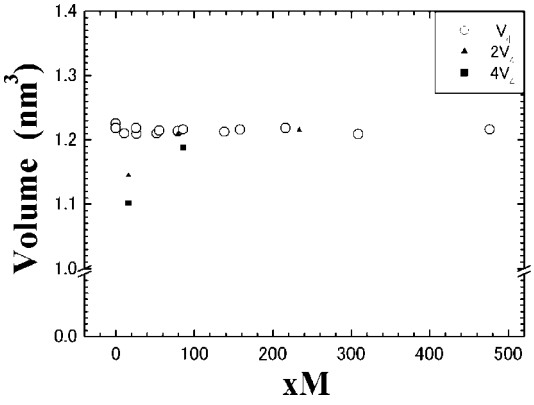

Figure 9. Mass effect such as lattice expansion is not seen in volume per [DEME][BF_4], V_4. x is concentration and M is atomic weight of each additions. Except for 0.9 mol % H_2O and 1.1 mol % C_6H_6, no distinct volume change is found in [DEME][BF_4]-based mixtures.

H_2O molecules probably cannot locate at the sublattice points simultaneously. Thus, we consider that a perfect order of additives is realized only at 1 mol %. Also, a medium-range order of additives can contribute to the elastic anomaly,

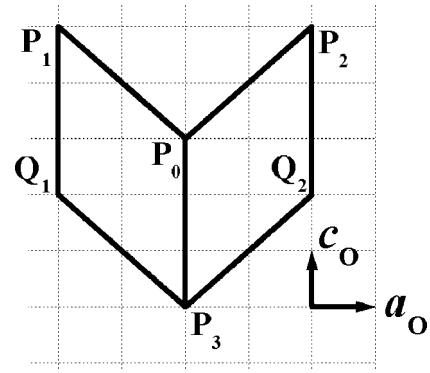

Figure 10. Geometrical relationship between the orthorhombic lattice and its sublattice is drawn on a_O-c_O plane. The sublattice is rhombic and the edge length of the rhombic is equal to $2b_O$.

supercell, and volume contractions at 0.9 mol % H_2O. The geometric effect is enhanced by additions of H_2O and C_6H_6, which may be derived from strong hydrogen bonding of H_2O and hydrophobic interaction of C_6H_6.

An additive effect in the [DEME][BF_4]−alcohol mixtures is quite small, since unit cell volume and crystal structures of the [DEME][BF_4]−alcohol mixtures are almost the same as those of pure [DEME][BF_4]. Below 10 mol %, hydrogen bonding of −OH is not so sensitive to the [DEME][BF_4] molecules.

In [DEME][BF_4]−C_6H_6 mixtures, different unit cell ($a'_M \times b'_M \times c'_M$) is required for the [DEME][BF_4]-based mixtures. In the previous studies,[6,13] the liquid structure in [C_1mim][PF_6]−C_6H_6 mixture suggests liquid clathrate formation, while the crystal structure in the mixture reveals a three-dimensional arrays of hydrogen-bonded cations and anions. In the three-dimensional network, each C_6H_6 molecule is separated. It has a tendency that C_6H_6 molecules distribute homogeneously and promote cation−cation interaction in both liquid and crystal states. In theoretical simulation,[14] it is pointed out that the quadrupole moment of a C_6H_6 molecule, which is providing the local electrostatic field, determines the arrangement of RTIL molecules even in dilute benzene−RTILs mixtures. In the [DEME][BF_4]−C_6H_6 mixtures, it is predicted that the major reorganization of cation−cation is induced by the additions. We confirm that the different crystal structure is realized by a balance between the reorganizations and molecular packing efficiency of the cations. Although a small amount of C_6H_6 molecules can form localized cage structure, reorganized cation ordering develops over the whole crystal.

5. Summary

Crystal structure reflects the molecular ordering. Two anomalous effects occur simultaneously only in 0.9 mol % H_2O and 1.1 mol % C_6H_6. One is two kinds of superstructures (symmetry breaking) and the other is volume contraction without stains in the specific mixtures. In particular, crystallization of the [DEME][BF_4]−0.9 mol % H_2O accompanies elastic anomaly considering formation of twinned domains. Furthermore, no lattice distortions are detected in the [DEME][BF_4]-based mixtures, though it is considered that lattice mismatches between $2V_4$ and $4V_4$ occur easily around their domain boundaries. Also, two kinds of superstructures suggest that two different kinds of water molecules exist obviously on crystallization.

Furthermore, only [DEME][BF_4]−C_6H_6 mixtures possess the different monoclinic crystal structure. Orientational or displacive ordering of [DEME][BF_4] molecules is quite different from other [DEME][BF_4]-based mixtures. Since the electrostatic field

around the benzene molecule is anisotropic, cations are strongly localized above and below the benzene rings. In spite of a small amount of C_6H_6, a localized cation−cation cluster sounding C_6H_6 molecule can form a different three-dimensional network.

Acknowledgment. We appreciate Ms. M. Sasaki and Mr. A. Kishi of Rigaku Co. for experimental support and helpful discussions. Also, the authors thank Professor H. Matsumoto and Professor T. Arai of National Defense Academy for helpful discussions.

References and Notes

(1) Earle, M. J.; Seddon, K. R. *Pure Appl. Chem.* **2000**, *72*, 1391.
(2) Hayashi, S.; Ozawa, R.; Hamaguchi, H. *Chem. Lett.* **2003**, *32*, 498.
(3) Saha, S.; Hayashi, S.; Kobayashi, A.; Hamaguchi, H. *Chem. Lett.* **2003**, *32*, 740.
(4) Ozawa, R.; Hayashi, S.; Saha, S.; Kobayashi, A.; Hamaguchi, H. *Chem. Lett.* **2003**, *32*, 948.
(5) Holbrey, J. D.; Reichert, W. M.; Nieuwenhuyzen, M.; Johnston, S.; Seddon, K. R.; Rogers, R. D. *Chem. Commun.* **2003**, 1636.
(6) Holbrey, J. D.; Reichert, W. M.; Nieuwenhuyzen, M.; Sheppard, O.; Hardacre, C.; Rogers, R. D. *Chem. Commun.* **2003**, 476.
(7) Hanke, C. G.; Lynden-Bell, R. M. *J. Phys. Chem. B* **2003**, *107*, 10873.
(8) Malham, I. B.; Letellier, P.; Turmine, M. *J. Phys. Chem. B* **2006**, *110*, 14212.
(9) Sato, T.; Masuda, G.; Takagi, K. *Electrochim. Acta* **2004**, *49*, 3603.
(10) Imai, Y.; Abe, H.; Goto, T.; Yoshimura, Y.; Kushiyama, S.; Matsumoto, H. *J. Phys. Chem. B* **2008**, *112*, 9841.
(11) Imai, Y.; Abe, H.; Goto, T.; Yoshimura, Y.; Michishita, Y.; Matsumoto, H. *Chem. Phys.* **2008**, *352*, 224.
(12) Gardon, M.; Pinheiro, C. B.; Chapuis, G. *Acta Crystallogr. B* **2003**, *59*, 527.
(13) Deetlefs, M.; Hardacre, C.; Nieuwenhuyzen, M.; Sheppard, O.; Soper, A. K. *J. Phys. Chem. B* **2005**, *109*, 1593.
(14) Harper, J. B.; Lynden-Bell, R. M. *Mol. Phys.* **2004**, *102*, 85.

JP808883P